Dendrochronology of Strain-Relaxed Islands

T. Merdzhanova,* S. Kiravittaya, A. Rastelli, M. Stoffel, U. Denker, and O. G. Schmidt

Max-Planck-Institut für Festkörperforschung, Heisenbergstrasse 1, D-70569 Stuttgart, Germany

(Received 19 December 2005; published 6 June 2006)

We report on the observation and study of tree-ring structures below dislocated SiGe islands (superdomes) grown on Si(001) substrates. Analogous to the study of tree rings (dendrochronology), these footprints enable us to gain unambiguous information on the growth and evolution of superdomes and their neighboring islands. The temperature dependence of the critical volume for dislocation introduction is measured and related to the composition of the islands. We show clearly that island coalescence is the dominant pathway towards dislocation nucleation at low temperatures, while at higher temperatures anomalous coarsening is effective and leads to the formation of a depletion region around superdomes.

DOI: 10.1103/PhysRevLett.96.226103 PACS numbers: 68.65.Hb, 68.37.Ps, 68.47.Fg, 81.15.Hi

The growth of self-assembled quantum dots using strained-layer epitaxy has attracted great interest in recent years due mainly to their potential applications in future nanoscale devices [1,2]. Among the different material combinations investigated so far, the Ge/Si(001) system is often used as a model for fundamental studies [3–6]. The growth follows the Stranski-Krastanow mode; i.e., it starts in a layer-by-layer mode up to a critical thickness of 3–4 monolayers (ML). At relatively high growth temperatures, the strain energy stored in the epilayer is partially relaxed via the formation of coherent islands, which undergo several transitions to steeper morphologies as their size increases [3–6]. For high Ge coverages, plastic relaxation of the growing epilayer occurs and large dislocated islands (also called ''superdomes'') are observed [7–10]. Until now, most efforts have been dedicated to the growth and the properties of coherent islands, since they are promising candidates for functionalization in novel device architectures. In contrast, much less work has been done to understand the growth and evolution of dislocated islands [7–15]. Remarkably, a cyclic growth mode was identified using *in situ* transmission electron microscopy (TEM) [7,8]. By using this technique, different pathways for dislocation nucleation were identified in the temperature range 350–650 °C during Ge growth on both Si(001) and Si(111) substrates [7,8,14].

In this Letter, we use a recently developed and much easier technique, compared to TEM, to trace the evolution of the dislocated and coherent islands by the analysis of their ''footprints'' left over on the surface. This technique combines selective wet chemical etching and atomic force microscopy (AFM) and has been successfully used to investigate the evolution of coherent islands [16,17]. Using wet chemical etching of the SiGe layer, we reveal a tree-ring structure below dislocated SiGe islands. This allows us to distinguish clearly dislocated from coherent islands and measure, with high statistics, the island volumes. While it is well known that such a volume should increase with the temperature [18], we are not aware of any study in which the critical volume for dislocation introduction was measured and directly related to the composition. A similar study is available only for the pyramid-to-dome transition [19]. We show that coalescence plays an important role at the lowest growth temperature investigated here (620 °C), while at higher temperatures anomalous coarsening is efficient and leads to the formation of a depletion region around the superdomes [6,9]. Another proof of the efficient role played by ripening in preventing island coalescence is the observation of shrinking islands close to large islands at high temperature (800 °C).

The samples studied in this work were grown by solid-source molecular beam epitaxy on Si(001) substrates. After deoxidation at 950 °C, the substrate temperature was ramped down to 460 °C, and a 100 nm thick Si buffer layer was grown at a rate of 0.1 nm/s. After a 5 s growth interruption, 15 ML of Ge were deposited at a rate of 0.04 ML/s at a substrate temperature between 620 and 800 °C. The morphology *of the same surface area* prior to and after 2 minutes etching in a buffered hydrofluoric acid, hydrogen peroxide, acetic acid solution [BPA solution, HF (1), H_2O_2 (2), CH_3COOH (3)] was characterized by *ex situ* AFM in tapping mode. The BPA solution is known to etch selectively $Si_{1-x}Ge_x$ alloys over pure Si [20,21].

Figures 1(a) and 1(b) show AFM images obtained upon deposition of 15 ML of Ge on Si(001) at 620 °C and 740 °C, respectively. In both samples, one can recognize different island morphologies such as coherently strained multifaceted islands [5,6,10] and some large superdomes. The main difference between the two samples is the island size, which increases with temperature mainly as a result of larger Si-Ge intermixing. AFM images obtained after etching are shown in Figs. 1(c) and 1(d) for the same surface areas shown in Figs. 1(a) and 1(b). The small sized islands leave behind circular Si plateaus surrounded by approximately square trenches with edges along the [100] and [010] directions as reported previously [21,22]. Surprisingly, the large islands leave behind a more complex footprint on the surface. It consists of several nearly concentric, irregular rings surrounding a central plateau. The rings are

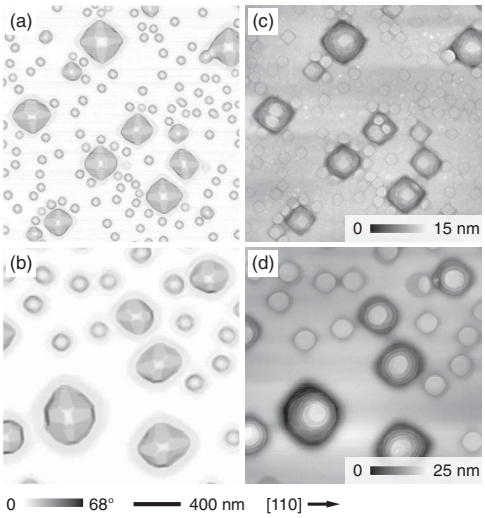

FIG. 1. AFM images taken after deposition of 15 ML Ge at 620 °C and at 740 °C before [(a) and (b), respectively] and after [(c) and (d), respectively] etching in a BPA solution. The color scales in the left and right panels correspond to slope and height, respectively.

located below the level of the flat Si surface, while the inner Si plateau is on average by 1 nm higher than the substrate surface [21]. Interestingly, some islands leave behind only one plateau, while some others leave behind several neighboring circular plateaus all surrounded by nearly concentric rings [Fig. 1(c)]. This result demonstrates that superdomes, which are comparable in size, can follow different pathways during their evolution. A comparison of the AFM images in Figs. 1(c) and 1(d) suggests already that different mechanisms of dislocation nucleation probably take place depending on the growth temperature.

In the following, we will focus on the evolution of the tree-ring structure left behind by the superdomes. A high resolution AFM scan of such a structure is shown in Fig. 2(a). Several rings surround the central Si plateau. Figure 2(b) represents a cross-sectional profile of the same superdome prior to (upper line scan) and after etching (middle line scan). The bottommost curve represents the second derivative of the AFM profile obtained after etching. The latter allows a clear identification of the rings position. Seven rings, pointed out by solid triangles, can be identified. The tree-ring structure, which is revealed by the etching, can be understood by considering the results of Refs. [7,8] and with reference to the simple phenomenological model depicted in Fig. 2(c). The left panel shows the edge of a coherent island on top of a thin wetting layer. During growth at sufficiently high temperatures, trenches surround the base of the islands [21,22]. Once a dislocation has been introduced, the island becomes a sink for material because it is more strain-relaxed and thus rapidly expands in a lateral direction, covering a part of the original trench. The part of the trench that is covered during the lateral growth is preserved, while the part that remains on the

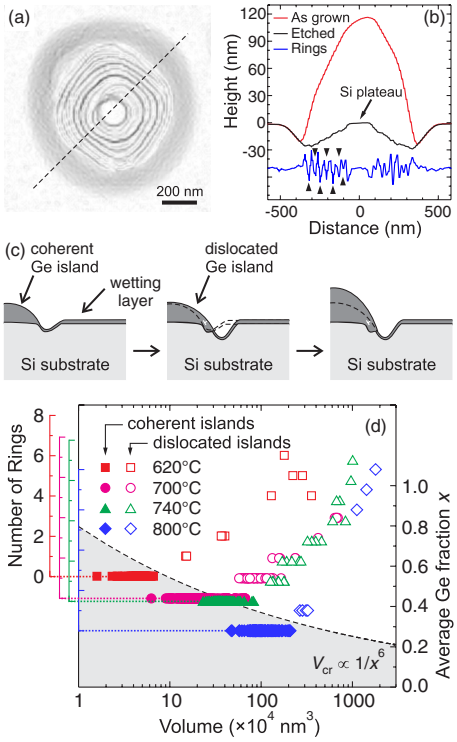

FIG. 2 (color online). (a) AFM scan of the tree-ring structure left over by a single superdome (grown at 800 °C) after etching. (b) Cross-sectional profile of the same superdome before and after etching taken along the dashed line shown in (a). The bottommost curve represents the numerical second derivative (in arbitrary units) of the AFM topograph of the profile after etching. The solid triangles indicate the position of the rings. (c) Schematic representation of the mechanism leading to the formation of ring structure. (d) Number of rings vs island volume for different temperatures. Note that the scatter plots of the number of rings are vertically shifted by a constant factor proportional to the estimated average Ge fraction x.

surface is subject to further erosion. Until nucleation of another dislocation, the island increases in size and creates thus a stress concentration at the newly formed island base that leads to the formation of a new, deeper trench. This process is repeated for each additional dislocation and results in the tree-ring structure observed in the experiment [see Figs. 1(c) and 1(d)]. We can thus interpret the number of rings as the number of dislocations introduced in the island during its growth, and, hence, we can gain information about the morphological age of the island. For example, the superdome shown in Fig. 2(a), with a base width of ~750 nm, contains 7 dislocations. Its average Ge fraction is 0.28 (see below), corresponding to a misfit of ~1.2%. If we assume 60°-type dislocations (commonly observed for the growth temperatures used here [7,8]), we find that the residual strain in the superdome is ~0.95%; i.e., the dislocations relieve ~20% of the misfit strain. Additional strain relaxation is provided by the steep morphology [23]. The absence or presence of a ring informs us whether islands are still coherent or already dislocated.

Figure 2(d) shows the evolution of the number of rings as a function of the island volume for different growth temperatures ranging from 620 to 800 °C. For each temperature considered, the number of rings first equals zero (a coherent island) and then increases with increasing island volume. We can thus define a critical volume V_{cr} for which it becomes energetically favorable for the island to incorporate a dislocation. The latter depends strongly on temperature; i.e., it increases when the growth temperature increases. This evolution suggests that Si-Ge intermixing plays a significant role. Indeed, when the growth temperature increases, the Si content increases [18,19,24], reducing the strain and delaying thus the introduction of dislocations. In order to estimate the average Ge fraction x in the islands, we measured the total volume of material per unit area from the AFM images and compared it with the nominally deposited Ge amount. Assuming that the critical volumes are proportional to x^{-6} [23,25], we can superimpose the evolution of the average Ge fraction to the evolution of the number of rings versus island volume [see Fig. 2(d)]. We can observe clearly that the decreasing Ge fraction follows almost the same trend as the evolution of the critical volume, demonstrating thus that a significant Si-Ge intermixing at high temperatures is indeed able to delay the introduction of dislocations.

The formation of dislocated islands may also be influenced by other phenomena. In order to get a better insight into the different processes that govern the nucleation of dislocations, we have measured the plateau width for both dislocated and coherent islands. Figure 3(a) displays the relative ratio of the plateau width of dislocated and coherent islands as a function of growth temperature. At low temperatures (620–700 °C), the plateau width of the coherent islands [$P_{coh} = 41 \pm 5$ nm at 620 °C; see, e.g., inset in Fig. 3(a)] is comparable to the plateau width of the dislocated islands [$P_{disl} = 44 \pm 6$ nm at 620 °C]. In contrast, for higher growth temperatures (740–800 °C), the plateau width of the dislocated islands appears significantly smaller than the plateau width of the coherent ones. We can suggest the following scenario: At sufficiently high temperatures, the islands can evolve by following two pathways. They can either intermix with Si or grow by the introduction of dislocations. In the former case, a higher Si intermixing will increase the base area and, consequently, the width of the buried plateau below the coherent islands. In the latter case, a tree-ring structure will form and the original plateau will not increase its width. It appears, therefore, smaller than the plateau buried below the coherent islands. A careful analysis of the footprints left over by the dislocated islands at low temperatures (620 °C) reveals an additional phenomenon. In some cases, not only one but several circular plateaus are buried below a single island [see Fig. 1(c)]. We interpret these features as being the result of island coalescence. Figure 3(b) shows the evolution of the ratio between the number of coalesced

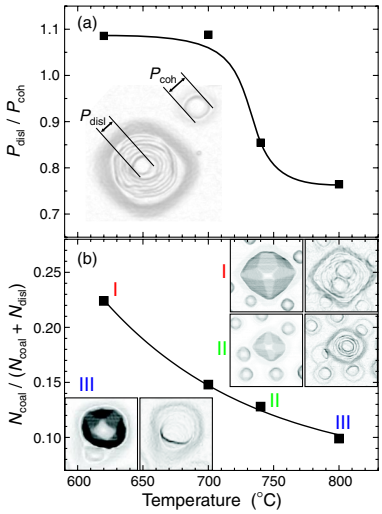

FIG. 3 (color online). (a) Relative ratio P_{disl}/P_{coh} vs growth temperature. P_{disl} and P_{coh}, defined in the inset, represent the plateau width of dislocated and coherent islands, respectively. (b) Effect of the growth temperature on the relative ratio of the number of coalesced and the number of dislocated islands. Insets: AFM scans of coherent and dislocated islands before and after etching, demonstrating the different processes related to dislocation formation: (I) island coalescence, (II) lateral motion triggered by island repulsion, and (III) material migration from smaller islands to larger neighbors.

islands and the total number of dislocated islands as a function of growth temperature. It is obvious that the number of coalesced events decreases when the growth temperature increases. This observation can be understand in terms of anomalous coarsening. Figure 4 shows two large area AFM scans of 15 ML Ge grown at 620 °C [Fig. 4(a)] and 740 °C [Fig. 4(b)], respectively. At 620 °C, the superdomes are surrounded by coherent islands [see inset in Fig. 4(a)], while an island depletion region is evident around the superdomes grown at 740 °C [see circle pointed at by an arrow in Fig. 4(b)]. To quantify this observation, we define Voronoi cells around both coherent and dislocated island centers and measure their corresponding area. The cell area, normalized by the average value for coherent islands, is plotted vs the island volume in Figs. 4(c) and 4(d) for the samples grown at 620 and 740 °C, respectively. Locally averaged values are also indicated with open symbols. We observe a marked increase of the Voronoi cell area for the superdomes contained in the sample grown at a higher temperature. The presence of a depletion region [9] can be explained as due to an anomalous coarsening process [17,26], in which the strain-relaxed superdomes grow at the expense of nearby smaller islands. At the highest temperature investigated here, we observe indeed very small shrinking islands which are being ''captured'' by larger and steeper islands, as illustrated in inset III [Fig. 3(b)]. Such a shrinking process is probably inefficient at relatively low temperatures, due

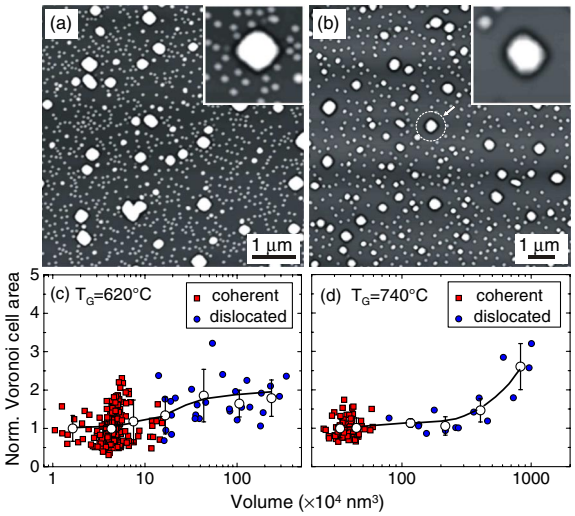

FIG. 4 (color online). AFM images of SiGe islands obtained after deposition of 15 ML Ge on Si(001) at (a) 620 °C and (b) 740 °C. A depletion region is evident around the dislocated islands in (b), while none is observed in (a); Voronoi cell area, normalized by the average value for coherent islands, vs island volume for (c) 620 °C and (d) 740 °C. Average values are plotted with open symbols. Lines are guides to the eye.

to the presence of a barrier for adatom detachment which is higher than the barrier for adatom attachment [27]. Therefore, we argue that, at low temperatures (620–700 °C), island coalescence and consequent dislocation introduction is more likely than island capture. Inset I in Fig. 3(b) shows a superdome which results from the coalescence of two islands. A tree-ring structure appears around the coalesced islands. In addition, our footprint analysis reveals that some coherent islands move away from the nearby superdomes [16,28]. A similar observation was reported during the growth of Ge on Si(111) substrates [14]. This phenomenon is observed throughout the whole temperature range investigated here and is probably due to strain mediated repulsion [28]. We expect that the Si incorporation resulting from the lateral motion will hinder or at least delay the coalescence. Such a type of process is illustrated in inset II [Fig. 3(b)] by the presence of a ''half-moon'' plateau under the moving island [16].

In conclusion, we have applied a selective etching method to reveal the footprints left over by superdomes. A complex tree-ring structure was identified, each ring corresponding to a dislocation. The analysis of the footprints enables us to gain a deeper insight into the evolution and the morphological age of superdomes. In particular, we identify island coalescence at the lowest temperature investigated in this study (620 °C) and island growth driven by anomalous coarsening at higher temperatures as different pathways for dislocation nucleation. We expect that our work provides a better understanding of the fundamental mechanisms governing the evolution of self-assembled islands in different strained material systems.

The authors thank A. Marzegalli, F. Montalenti, and Leo Miglio for fruitful discussions and K. von Klitzing for his continuous support and interest. The work was supported by the BMBF (03N8711) and EU (012150).

*Electronic address: t.merdzhanova@fkf.mpg.de

[1] O. G. Schmidt and K. Eberl, IEEE Trans. Electron Devices **48**, 1175 (2001).
[2] Z. Yuan, B. E. Kardynal, R. M. Stevenson, A. J. Shields, C. J. Lobo, K. Cooper, N. S. Beattie, D. A. Ritchie, and M. Pepper, Science **295**, 102 (2002).
[3] A. Vailionis, B. Cho, G. Glass, P. Desjardins, D. G. Cahill, and J. E. Greene, Phys. Rev. Lett. **85**, 3672 (2000).
[4] Y. W. Mo, D. E. Savage, B. S. Swartzentruber, and M. G. Lagally, Phys. Rev. Lett. **65**, 1020 (1990).
[5] G. Medeiros-Ribeiro, A. M. Bratkovski, T. I. Kamins, D. A. A. Ohlberg, and R. S. Williams, Science **279**, 353 (1998).
[6] F. M. Ross, R. M. Tromp, and M. C. Reuter, Science **286**, 1931 (1999).
[7] F. K. LeGoues, M. C. Reuter, J. Tersoff, M. Hammar, and R. M. Tromp, Phys. Rev. Lett. **73**, 300 (1994).
[8] M. Hammar, F. K. LeGoues, J. Tersoff, M. C. Reuter, and R. M. Tromp, Surf. Sci. **349**, 129 (1996).
[9] T. I. Kamins, G. Medeiros-Ribeiro, D. A. A. Ohlberg, and R. S. Williams, J. Appl. Phys. **85**, 1159 (1999).
[10] A. Rastelli and H. von Känel, Surf. Sci. Lett. **515**, L493 (2002).
[11] J. Tersoff and R. M. Tromp, Phys. Rev. Lett. **70**, 2782 (1993).
[12] H. T. Johnson and L. B. Freund, J. Appl. Phys. **81**, 6081 (1997).
[13] B. J. Spencer and J. Tersoff, Phys. Rev. B **63**, 205424 (2001).
[14] F. K. LeGoues, M. Hammar, M. C. Reuter, and R. M. Tromp, Surf. Sci. **349**, 249 (1996).
[15] Y. Hiroyama and M. Tamura, J. Vac. Sci. Technol. A **16**, 2956 (1998).
[16] U. Denker *et al.*, Phys. Rev. Lett. **94**, 216103 (2005).
[17] A. Rastelli *et al.*, Phys. Rev. Lett. **95**, 026103 (2005).
[18] D. J. Smith, D. Chandrasekhar, S. A. Chaparro, P. A. Crozier, J. Drucker, M. Floyd, M. R. McCartney, and Y. Zhang, J. Cryst. Growth **259**, 232 (2003).
[19] M. Floyd and Y. Zhang, Appl. Phys. Lett. **82**, 1473 (2003).
[20] T. K. Carns *et al.*, J. Electrochem. Soc. **142**, 1260 (1995).
[21] U. Denker *et al.*, Appl. Phys. Lett. **78**, 3723 (2001).
[22] S. A. Chaparro, Y. Zhang, J. Drucker, D. Chandrasekhar, and D. J. Smith, J. Appl. Phys. **87**, 2245 (2000).
[23] J. A. Floro, G. A. Lucadamo, E. Chason, L. B. Freund, M. Sinclair, R. D. Twesten, and R. Q. Hwang, Phys. Rev. Lett. **80**, 4717 (1998).
[24] T. U. Schülli *et al.*, Phys. Rev. B **71**, 035326 (2005).
[25] A. Rastelli *et al.*, Phys. Rev. Lett. **87**, 256101 (2001).
[26] F. M. Ross, J. Tersoff, and R. M. Tromp, Phys. Rev. Lett. **80**, 984 (1998).
[27] A.-L. Barabási, Appl. Phys. Lett. **70**, 2565 (1997).
[28] M. Stoffel *et al.*, Phys. Rev. B **72**, 205411 (2005).